19th Brazilian Congress of Thermal Sciences and Engineering
November 6th–10th, 2022, Bento Gonçalves - RS - Brazil

ENC-2022-0466
NUMERICAL INVESTIGATION OF FERROFLUID DROPLETS MOTION IN PRESSURE DRIVEN FLOWS

Rogério Ghiraldeli Botelho De Paula
Taygoara Felamingo de Oliveira
Energy and Environment Laboratory, Department of Mechanical Engineering, University of Brasilia, Brasilia, DF, Brazil
rogerghira@gmail.com
taygoara@unb.br

Abstract. *In this work, the motion of ferrofluid droplets dispersed in a pressure-driven flow under the influence of an external magnetic field is studied using numerical methods. The model assumes droplets of superparamagnetic fluids dispersed in a non-magnetizable Newtonian media between two parallel plates in incompressible laminar pressure-driven flow, affected by an external uniform magnetic field. We solve the incompressible Navier-Stokes equations, with additional source terms representing the pressure jump due to the surface tension and the magnetic forces inside the droplet, couplet to a Laplace equation for the magnetic potential. The numerical methodology uses the Level Set method to capture the droplet surface and the projection method for the pressure-velocity coupling. The MAC second-order finite differences scheme is used for spatial discretization and the Crank-Nicholson method is applied to the temporal evolution of the momentum equation. High order ENO and WENO conservative schemes are used for the solution of the Level Set equations. Inertia effects are minimized by keeping a low Reynolds number. In this limit, the main parameters of the problem are the capillary number (Ca), accounting for the ratio between the shear stress and the surface tension; and the magnetic capillary number (Ca_{mag}), which is the external magnetic field intensity normalized using the surface tension. We present a numerical study on the influence of the external magnetic field on the drift velocity of the droplets. It is observed that droplets placed near the wall tend to migrate towards the center, showing that droplets migrate to regions with less intense shear rates and migrates faster with larger deformation in the presence of a magnetic field.*

Keywords: *Pressure Driven, ferrofluid, Numerical analysis, Emulsion*

1. INTRODUCTION

Predicting motion of liquid drops through narrow channels is a challenging problem that is relevant to technological, biological and natural phenomena Olbricht (1996). In engineering, we have the flow of liquid droplets in a porous medium in oil recovery Olbricht (1996). On the biological side, there is the flow of red blood cells through narrow spaces in capillary tubes Skalak *et al.* (1989). Because the distribution of drops through the cross-section of the channel determines the flow rate, for a given pressure drop, determining the lateral migration of the drops and their final equilibrium position is of particular interest.

There is a wide range of applications supporting the growing research on the behavior of ferrofluid droplets as magnetically controllable fluids, as shown by Torres-Díaz and Rinaldi (2014). Some applications involve the interaction with an external magnetic field, for example in biomedical processes, such as target drug delivery and restorative treatment of retinal detachment. Cunha and Sobral (2004) have studied the flow of a mono phase magnetic fluid in a pressure-driven flow, they proposed a slightly non-linear theory which allows the definition the volume rate in terms of the applied field.

Cox and Brenner (1968) published a paper the theory of lateral migration of solid particles. They presented the theory for migration in laminar flows through vertical tubes of circular and non-circular cross-section and studied cases with neutrally and non-neutrally buoyant particles. It is used the idea of separating both the velocity and pressure terms into the sum of a constant and a disturbance terms. Cox and Hsu (1977) continued the work on this line of field and published a paper utilizing the results from the previous work to calculate analytically the migration velocity of a spherical particle in a flow near a single vertical plane.

Droplets lateral migration in a Poiseuille flow has been observed if in absence droplet deformation, surfactants or fluid viscoelasticity, in Stokes flow limit. Mortazavi and Tryggvason (2000) have shown in a numerically 2D Poiseuille flow, that a droplet under the low-Reynolds-number limit with low viscosity ratio always migrates towards the centreline of the

channel. Whereas, for an unit viscosity ratio, the drop moves away form the centreline.

Kaoui *et al.* (2008) performed studies of lateral migration of a two-dimensional vesicle in a Poiseuille flow in the low Reynolds number limit. Using boundary integral method to solve the flow equations and tracking the vesicle explicitly. It was found that the interplay between the Poiseuille flow and the vesicle deformation causes a cross-streamline migration of vesicles toward the center of the Poiseuille flow. This result is contrary to what other authors found which the droplet moves away from the center, in similar conditions.

Liu *et al.* (2012) utilized a Lattice Boltzmann multiphase model to understand how thermocapillary forces manipulate droplet motion in microfluidic channels. The complex hydrodynamic interactions are described by an improved color-fluid LB model, in which the interfacial tension forces and the Marangoni stresses are modeled in a consistent manner using the concept of a continuum surface force. An additional convection–diffusion equation is solved in the LB framework to obtain the temperature field, which is coupled to the interfacial tension through an equation of state. The model is firstly validated against the analytical solutions for the thermocapillary driven convection in two superimposed fluids at negligibly small Reynolds and Marangoni numbers.

Liu *et al.* (2013) developed a phase-field-based hybrid model that combines the lattice Boltzmann method with the finite difference method proposed for simulating immiscible thermocapillary flows with variable fluid-property ratios. Using a phase field methodology, an interfacial force formula is analytically derived to model the interfacial tension force and the Marangoni stress. An additional convection-diffusion equation is solved by the finite difference method for spatial discretization and the Runge-Kutta method for time marching to obtain the temperature field, which is coupled to the interfacial tension through an equation of state. It is then used to simulate thermocapillary migration of a three-dimensional deformable droplet and bubble at various Marangoni numbers and density ratios, and satisfactory agreement is obtained between numerical results and theoretical predictions.

Hood *et al.* (2013) studied the inertial migration of a rigid sphere in three-dimensional Poiseuille flow. Inertial lift forces are exploited within inertial microfluidic devices to position, segregate and sort particles or droplets. However, the forces and their focusing positions can currently only be predicted by numerical simulations, making rational device design very difficult. A theory was developed for the forces on particles in microchannel geometry. Numerical experiments were used to dissect the dominant balances within the Navier–Stokes equations and derive an asymptotic model to predict the lateral force on the particle as a function of particle size.

There also have been studies that have shown how droplets interact with a interface of a three-phase system. The flow is composed of two immiscible streams in a microchannel and the dispersed phase. Hazra *et al.* (2022) have found that small droplets migrates towards the interface, while larger ones drift away from the interface. Numerical simulations revealed that interfacial deformation is a consequence of pressure jumps across the interface of the main phases at the upstream and downstream of a droplet.

The use of external effects such as electric (Ahn *et al.* (2006) and Mandal *et al.* (2016)), thermal (Young *et al.* (1959) and Das *et al.* (2018)), acoustic (Seemann *et al.* (2011)) and magnetic (Seemann *et al.* (2011)) have been studied due to the necessity of controlling the droplet migration. Das *et al.* (2018) have studied the effect of temperature gradient on the migration of a Poiseuille flow. Their problem cannot be simply described as a superposition of the influences of the flow components due to thermocappilary and the pressure-driven flow.

Since the flow over a channel or a tube takes some distance to fully develop, it is necessary a large computational domain in order to obtain a simulation for a single drop migration. However, this large domain is not needed if a periodic boundary condition is applied in the direction of the flow, providing fewer points on the computational domain that need to be solved.

In this work, the motion of ferrofluid droplets dispersed in a pressure-driven flow under the influence of an external magnetic field is studied using numerical methods. For this, we consider a two-dimensional domain, with a single ferrofluid dispersed in a non-magnetizable Newtonian media between two parallel plates in incompressible laminar pressure-driven flow, affected by an external uniform magnetic field. The numerical methodology uses the Level Set method to track the droplet surface and the projection method for the pressure-velocity coupling. The MAC second-order finite differences scheme is used for spatial discretization and the Crank-Nicholson method is applied to the temporal evolution of the momentum equation. High order ENO and WENO conservative schemes are used for the solution of the Level Set equations.

We have found that the droplet migrates towards the centerline due to the velocity gradient. In the presence of an external vertical magnetic field, the droplet undergoes large deformations and experiences a faster migration towards the center while experiencing a flapping motion.

2. PROBLEM STATEMENT

Figure 1 show a schematic representation of the problem. We consider a single superparamagnetic droplet in an immiscible flow, non-magnetizable fluid media between two parallel plates in incompressible laminar pressure-driven flow, affected by an external uniform magnetic field. The plates are normal to the y-direction and periodic in the x-direction. Both phases have the same density ρ and viscosity η. The continuous phase has magnetic permeability μ_0 equal

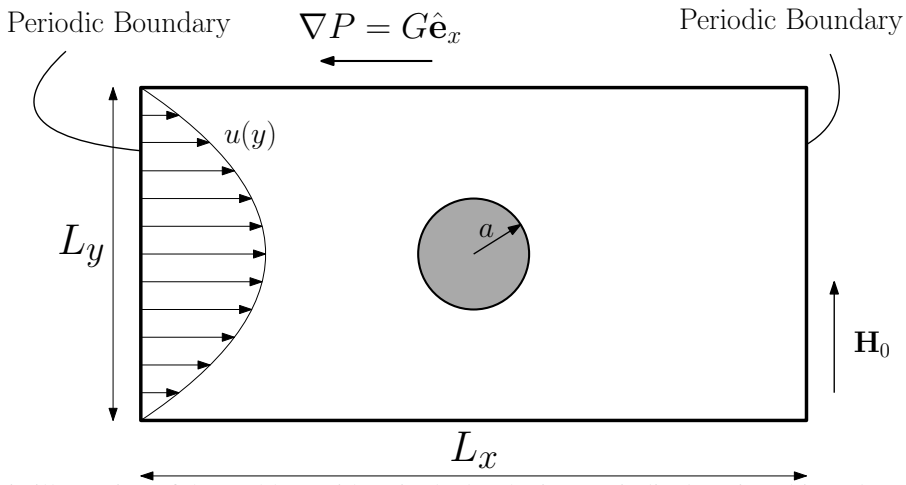

Figure 1: Schematic illustration of the problem with a single droplet in a periodic domain subjected to a pressure gradient G in the x-direction.

to free space magnetic permeability. The ferrofluid droplet has magnetic permeability of $\zeta\mu_0$, where ζ represents the ratio between the dispersed and continuous phases magnetic permeability. The surface tension σ is constant, we assume the surface of the droplet to be free of tensioactive substances. The system is subjected to a constant gradient of pressure G that drives the flow, similar to a Hagen-Poiseuille flow. The system is also subjected to an external magnetic field $\mathbf{H}_0$, which can be parallel to the x- or y- direction, the main flow direction and the main vorticity direction.

In the absence of electric current, Maxwell's equations are reduced to $\nabla \cdot \mathbf{B} = 0$ and $\nabla \times \mathbf{H} = 0$, where $\mathbf{B}$ is the magnetic induction and $\mathbf{H}$ the magnetic field. Due to the superparamagnetic assumption, the magnetization of the droplet follows the relation $\mathbf{M} = \chi\mathbf{H}$, where χ is the magnetic susceptibility. The magnetic induction has a contribution of the material magnetization and the magnetic field, so that $\mathbf{B} = \mu_0 (\mathbf{M} + \mathbf{H})$. This leads to $\mathbf{B} = \mu_0 (1 + \chi) \mathbf{H}$ inside the droplet, and $\mathbf{B} = \mu_0\mathbf{H}$ outside of it, so we define a continuous function $\zeta_\phi(\mathbf{x})$ such that $\zeta_\phi(\mathbf{x}) = 1$ outside of the droplet and $\zeta_\phi(\mathbf{x}) = 1 + \chi$ in the inside of it. Since $\nabla \times \mathbf{H} = 0$, $\mathbf{H}$ can be written as a gradient of the magnetic potential ψ, such that $\mathbf{H} = -\nabla\psi$, and, since $\nabla \cdot \mathbf{B} = 0$, we arrive at

$$\nabla \cdot (\zeta_\phi(\mathbf{x})\nabla\psi) = 0, \tag{1}$$

which governs the magnetic part of the problem.

The hydrodynamic problem is governed by the incompressible Navier-Stokes equations with terms accounting the capillary and the magnetic forces per unit of volume, $\mathbf{F}_c$ and $\mathbf{F}_m$ respectively. The set of equations are

$$\rho \left(\frac{\partial \mathbf{u}}{\partial t} + \mathbf{u} \cdot \nabla \mathbf{u} \right) = -\nabla P + \eta \nabla^2 \mathbf{u} + \mathbf{F}_c + \mathbf{F}_m, \tag{2}$$

and

$$\nabla \cdot \mathbf{u} = 0, \tag{3}$$

where $\mathbf{u}$ is the velocity vector, t is the time, P is the pressure. We use the Level Set Method to create a signed distance function ϕ and track the interface at level $\phi = 0$. The capillary forces can be expressed using the level set function as

$$\mathbf{F}_c = -\sigma\kappa\delta(\phi) |\nabla\phi| \hat{\mathbf{n}}, \tag{4}$$

where κ is the mean curvature, δ is the Dirac delta distribution and $\hat{\mathbf{n}}$ is the normal vector pointing towards the outside of the droplet. The magnetic force term is calculated as

$$\mathbf{F}_m = \mu_0 [\zeta (\mathbf{x}) - 1] \mathbf{H} \cdot \nabla \mathbf{H}. \tag{5}$$

We use periodic boundary conditions because of the benefits of not needing a large computational domain to simulate flow in a channel. However, we can not apply the pressure gradient that drives the flow directly due to the periodic boundary, so we adapted the pressure gradient. The adaptation consist of splitting the gradient

$$\nabla P = (\nabla P)' + \mathbf{G}, \tag{6}$$

where $\mathbf{G} = G\hat{\mathbf{e}}_x$ is the applied pressure gradient, that drives the flow, and $(\nabla P)'$ is the component that enforces the incompressible restriction. Rewriting the Navier-Stokes equation,

$$\rho\left(\frac{\partial \mathbf{u}}{\partial t} + \mathbf{u}\cdot\nabla\mathbf{u}\right) = -(\nabla P)' + \eta\nabla^2\mathbf{u} + \mathbf{F}_c + \mathbf{F}_m - \mathbf{G}. \tag{7}$$

One can think of Eq. (7) as Navier-Stokes equations with a body force term $\mathbf{G}$, similar to flow in a vertical tube under the influence of gravity. The separation of variables helps in the implementation of the periodic boundary with only the need to solve for $(\nabla P)'$. For the sake of simplicity we will drop the apostrophe notation in further equations.

The boundary conditions of the magnetic part of the problem need attention due to the periodic boundaries, since there can not be a gradient of ψ in the x-direction. We consider a physical situation where the flow occurs in annular space between two concentric cylinders (Coutte flow), as shown in Fig. 2. In the center of the cylinders, a constant electrical current I passes through a conductor wire, generating a magnetic field H_0 in the flow. The ratio $\Delta R/R$ is small enough such that variations of $\mathbf{H}_0$ along the gap are negligible.

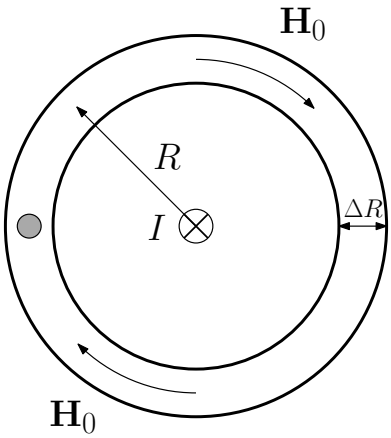

Figure 2: Schematic representation of an experiment with magnetic field generated by a constant current.

We will use a similar solution as we did with the pressure, separating $\mathbf{H} = \mathbf{H}' + \mathbf{H}_0$, where $\mathbf{H}_0$ is the external magnetic field and $\mathbf{H}'$ is the component that enforces the solenoidal condition. Applying the separation into Eq. (1)

$$\nabla\cdot[\zeta_\phi(\mathbf{x})\mathbf{H}' + \zeta_\phi(\mathbf{x})\mathbf{H}_0] = 0, \tag{8}$$

rearranging,

$$\nabla\cdot[\zeta_\phi(\mathbf{x})\mathbf{H}'] = -\nabla\cdot[\zeta_\phi(\mathbf{x})\mathbf{H}_0], \tag{9}$$

given that $\mathbf{H}_0$ is constant for the whole domain since is the applied field, it is simplified to

$$\nabla\cdot[\zeta_\phi(\mathbf{x})\mathbf{H}'] = -\nabla\cdot[\zeta_\phi(\mathbf{x})\nabla\psi] = -\mathbf{H}_0\cdot\nabla\zeta_\phi(\mathbf{x}). \tag{10}$$

One might ask what is $\mathbf{H}_0$, to answer that we use Biot-Savart law for the case which the external field is aligned with the flow direction and get $\mathbf{H}_0 = \mu_0 I/2\pi R\hat{\mathbf{e}}_x$, where we control the variables I and R. The advantage of using Eq. (10) is that the external field conditions are no longer applied to the boundaries of the domains, instead, they are applied everywhere but are different than zero at the interface between the two fluids.

The characteristic velocity of the problem is obtained by calculating the average velocity of a single phase Hagen-Poiseuille flow between to plates with a parabolic velocity profile. We use the following characteristics magnitudes

$$|\mathbf{u}_c| = \frac{GL_y^2}{12\eta}, \quad |(\nabla P)_c| = G, \quad L_c = L_y, \quad |\mathbf{H}_c| = |\mathbf{H}_0| \tag{11}$$

are used to obtain the non-dimensional form of the equations.

The non-dimensional governing Navier-Stokes equation is

$$\frac{\partial\tilde{\mathbf{u}}}{\partial\tilde{t}} + (\tilde{\mathbf{u}}\cdot\tilde{\nabla})\tilde{\mathbf{u}} = -\frac{12}{Re}\left(\tilde{\nabla P}\right) + \frac{1}{Re}\tilde{\nabla}^2\tilde{\mathbf{u}} - \frac{1}{CaRe}\tilde{\kappa}\tilde{\delta}(\tilde{\phi})\hat{\mathbf{n}} + \frac{Ca_{mag}}{ReCa}\left[\zeta(\mathbf{x}) - 1\right]\tilde{\mathbf{H}}\cdot\tilde{\nabla}\tilde{\mathbf{H}} + \frac{12}{Re}\hat{\mathbf{e}}_x, \tag{12}$$

where $Re = GL_y^3/12\eta\nu$ is the Reynolds number, $Ca = GL_y^2/12\sigma$ is the Capillary number, $Ca_{mag} = \mu_0\left|\mathbf{H}_0\right|^2/\sigma$.

For the sake of simplicity, we will suppress the tilde notation for the remainder of this text.

3. METHODOLOGY

3.1 Projection Method

We use the fractional projection method of Kim and Moin (1985) as presented by Brown *et al.* (2001) to solve the mass and momentum equations. It uses a second-order Crank-Nicolson scheme for the time step and a second-order Adams-Bashforth for the explicit terms to avoid non-linear terms on the future time step. First we solve for a intermediate velocity $\mathbf{u}^*$ in a similar equation to Eq. (12)

$$\frac{\mathbf{u}^* - \mathbf{u}^n}{\Delta t} = \frac{1}{2Re}\nabla_h^2 \left(\mathbf{u}^* - \mathbf{u}^n\right) + \mathbf{rhs}^{n+1/2}, \tag{13}$$

where $\mathbf{u}^n$ is the velocity vector field at time-step n, ∇_h is the discrete nabla operator and $\mathbf{rhs}^{n+1/2}$ are all the remaining on the right hand side of Eq. (12), with exception to the pressure gradient, extrapolated to time-step $n + 1/2$. Then we solve for a pseudo pressure $\hat{p}$

$$\nabla_h^2 \hat{p}^{n+1} = \nabla_h \cdot \mathbf{u}^*, \tag{14}$$

and then update the velocity and pressure terms like so

$$\mathbf{u}^{n+1} = \mathbf{u}^* - \Delta t \nabla_h \hat{p}^{n+1}, \tag{15}$$

$$P^{n+1} = \hat{p}^{n+1} - \frac{\Delta t}{2Re}\nabla_h \cdot \mathbf{u}^*. \tag{16}$$

The boundary conditions applied in the horizontal parallel plates. For $\mathbf{u}^*$ those are

$$\mathbf{u}^* \cdot \hat{\mathbf{n}} = 0, \tag{17}$$

$$\mathbf{u}^* \cdot \hat{\mathbf{t}} = \Delta \left(2\nabla_h \hat{p}^n - \nabla_h \hat{p}^{n-1}\right) \cdot \hat{\mathbf{t}}, \tag{18}$$

where $\hat{\mathbf{t}}$ is the unit tangent vector. For $\hat{p}$ those are

$$\nabla_h \hat{p} \cdot \hat{\mathbf{n}} = 0. \tag{19}$$

For ψ we apply Neumann conditions in the horizontal plates such that

$$\nabla_h \psi = -\mathbf{H}_0. \tag{20}$$

For the vertical parallel plates we apply periodic conditions.

The discretization of the domain is performed using a regular, staggered grid, with centered second-order finite differences with exception for the advective term, which uses a second-order essentially non-oscillatory (ENO) scheme with upwinding

3.2 Level Set Method

To track the interface and its topological changes we use the Level Set Method Sussman *et al.* (1998). We create a signed distance function ϕ to the interface, where $\phi < 0$ in the inside of the droplet, $\phi > 0$ outside of it and $\phi = 0$ at the interface. Since ϕ is a signed distance function, we can define the unit normal vector as $\hat{n} = \nabla\phi / |\nabla\phi|$ in all domain where $|\nabla\phi| \neq 0$, and the local mean curvature $\kappa = \nabla \cdot \hat{n} = \nabla \cdot (\nabla\phi / |\nabla\phi|)$.

The Level Set method uses smooth transitions across the interface. To create that, we adopt a finite thickness ε and define the smoothed Heaviside function as

$$H_\varepsilon(\phi) = \begin{cases} 0, & \text{if } \phi < -\varepsilon, \\ 1/2\left[1 + \frac{\phi}{\varepsilon} - \frac{1}{\pi}\sin\left(\pi\phi/\varepsilon\right)\right], & \text{if } |\phi| \leq \varepsilon, \\ 1, & \text{if } \phi > \varepsilon, \end{cases} \tag{21}$$

and the smoothed Dirac delta δ_ε as the derivative of H_ε such as

$$\delta_\varepsilon(\phi) = \frac{dH_\varepsilon(\phi)}{d\phi} = \begin{cases} 0, & \text{if } |\phi| > \varepsilon, \\ \frac{1}{2\varepsilon}\left[1 + \cos\left(\frac{\pi\phi}{\varepsilon}\right)\right], & \text{if } |\phi| \leq \varepsilon. \end{cases} \tag{22}$$

In our simulations we used $\varepsilon = \frac{3}{2}\Delta x$. We can rewrite the magnetic permeability as $\zeta_\phi(\phi) = \zeta + (1-\zeta)H_\varepsilon(\phi)$.

We evolve the motion of the interface by solving the Hamilton-Jacobi equation

$$\frac{\partial \phi}{\partial t} + \mathbf{u} \cdot \nabla \phi = 0, \tag{23}$$

which conserves the value of ϕ on fluid particles at the interface, but ϕ will generally diverge from the signed distance function and can cause miscalculations of the normal vector and curvature. Thus, we avoid this issue by applying a re-distancing procedure for every time-step. The method adopted was the same of Sussman and Fatemi (1999), solving the re-initialization equation

$$\frac{\partial \phi}{\partial \tau} + S(\phi)\left(|\nabla \phi| - 1\right) = \lambda \delta(\phi)\left|\nabla \phi\right|, \tag{24}$$

where τ is the virtual time-step, $S(\phi)$ is the sign function and λ is the Lagrange multiplier defined as

$$\lambda = \frac{\int_V \delta(\phi)\left(\frac{\phi^{n+1}-\phi^n}{\Delta t}\right) dV}{\int_V \delta^2(\phi)\left|\nabla \phi\right| dV}, \tag{25}$$

where the integral are taken in the whole domain V. The right hand side of Eq. (24) is a correction term to avoid numerical variations in the re-initialization step and preserve the interface, if no correction is needed, the integral in the numerator of equation Eq. (25) goes to zero.

4. RESULTS AND DISCUSSION

For all cases presented in this work, we use a domain size of 2×1 (with $-1 < x < 1$ and $-0.5 < y < 0.5$) and a mess discretization of 256×128. We fix the parameters $Re = 1$ and $\zeta = 2$. The droplet has a circular shape of radius $r = 0.2$, this corresponds to a volume fraction $\beta \approx 6\%$.

To verify if the implementation of the magnetic forces is done correctly, first we check the deformation of a droplet in the presence of an external vertical magnetic field without the presence of pressure gradient. Figure 3 shows the stretching effect comparing the difference the initial condition and the stretched droplet at time $t = 6.6$.

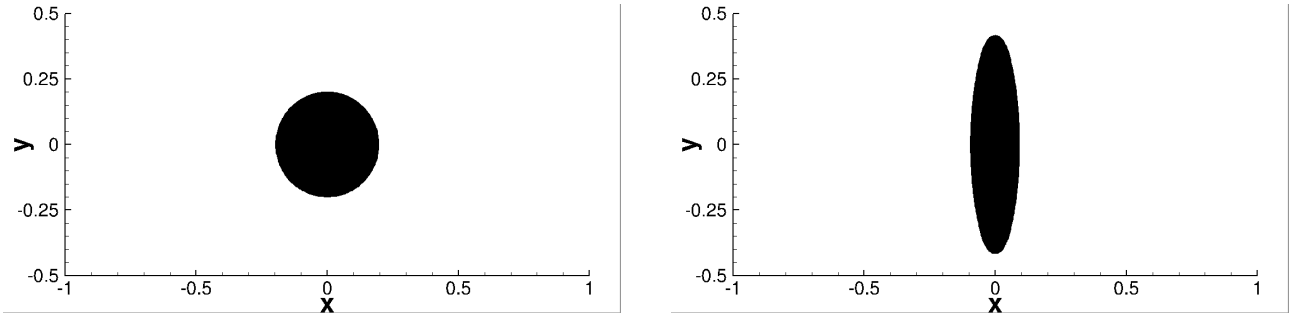

(a) Initial condition (b) $t = 6.60$

Figure 3: Droplet deformation due to an external magnetic field in the vertical direction without pressure gradient. $Re = 1$, $Ca = 0.5$ and $Ca_{mag} = 8$. (An animation can be seen by clicking here or in the link: `https://youtu.be/I2RowkwEQ40`)

We verify the motion of the droplet in a pure pressure driven flow without magnetic fields. Figure 4 shows the droplet after reaching steady state of deformation with initial condition as the same as Fig. 3a.

The migration of the droplet is studied by initializing the droplet with center located in $(0, -0.15)$ with radius $r = 0.2$, these parameters are arbitrary and chosen such that the droplet is not so close to the wall and still far from the center. Figure 5 shows the shape of the droplet in at initial condition and after some time, without the external magnetic field.

In the presence of the external magnetic field, the droplet undergoes to large deformation. This happens because the vertical magnetic field tends to elongate the droplet in the vertical direction, and thus is subjected to a larger velocity gradient. Figure 6 shows the droplet at time $t = 60$ for various magnetic capillary numbers with initial condition as the same as Fig. 5a. The higher the Ca_{mag} the larger deformation in the vertical direction.

Figure 7 show the motion of the droplet in various timesteps for $Ca_{mag} = 1$. The droplet under goes large deformations and assumes a shape similar to a stingray and does not remain stationary. It is observed a flapping motion on the tips of the droplet. This observations are valid for all magnetic capillary numbers simulated with higher Ca_{mag} leading to a more vertical shape.

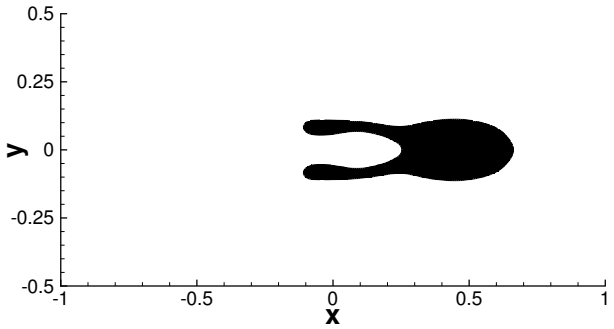

Figure 4: Droplet under pure pressure driven flow without magnetic field after reaching steady state. $Re = 1$ and $Ca = 0.5$

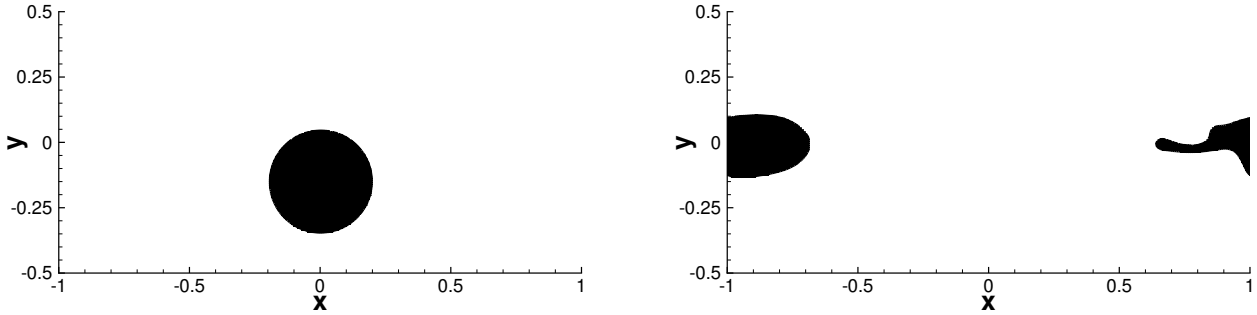

(a) Initial condition

(b) $t = 60$

Figure 5: Droplet migration in a pressure driven flow without the presence of external magnetic field ($Ca_{mag} = 0$). $Re = 1$, $Ca = 0.5$. (An animation can be seen by clicking **here** or in the link: `https://youtu.be/y0Q5SJWomwk`)

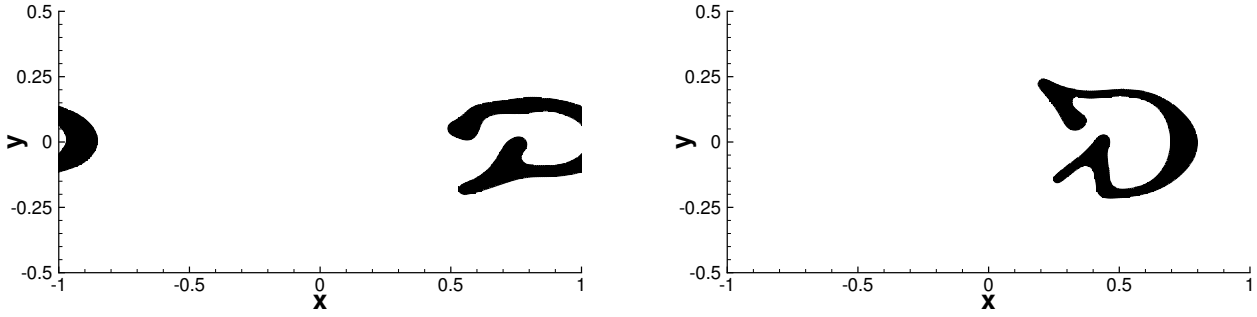

(a) $Ca_{mag} = 1$

(b) $Ca_{mag} = 2$

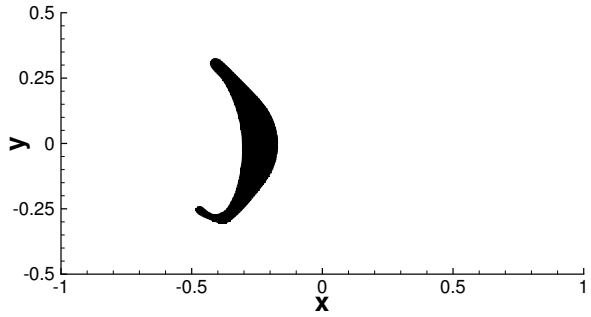

(c) $Ca_{mag} = 4$

Figure 6: Droplet migration at time $t = 60$ in a pressure driven flow with $Ca_{mag} = 1$, $Ca_{mag} = 2$ and $Ca_{mag} = 4$. $Re = 1$, $Ca = 0.5$ (An animation for each case can be seen by clicking $Ca_{mag} = 1$, $Ca_{mag} = 2$, $Ca_{mag} = 4$)

In order to better analyze the motion of the droplet, we record the compute the location of the droplet's center of gravity with

$$\mathbf{x}_{cg} = \frac{\int_V \mathbf{x}\,[1 - H_\varepsilon(\phi)]\,dV}{\int_V [1 - H_\varepsilon(\phi)]\,dV}, \tag{26}$$

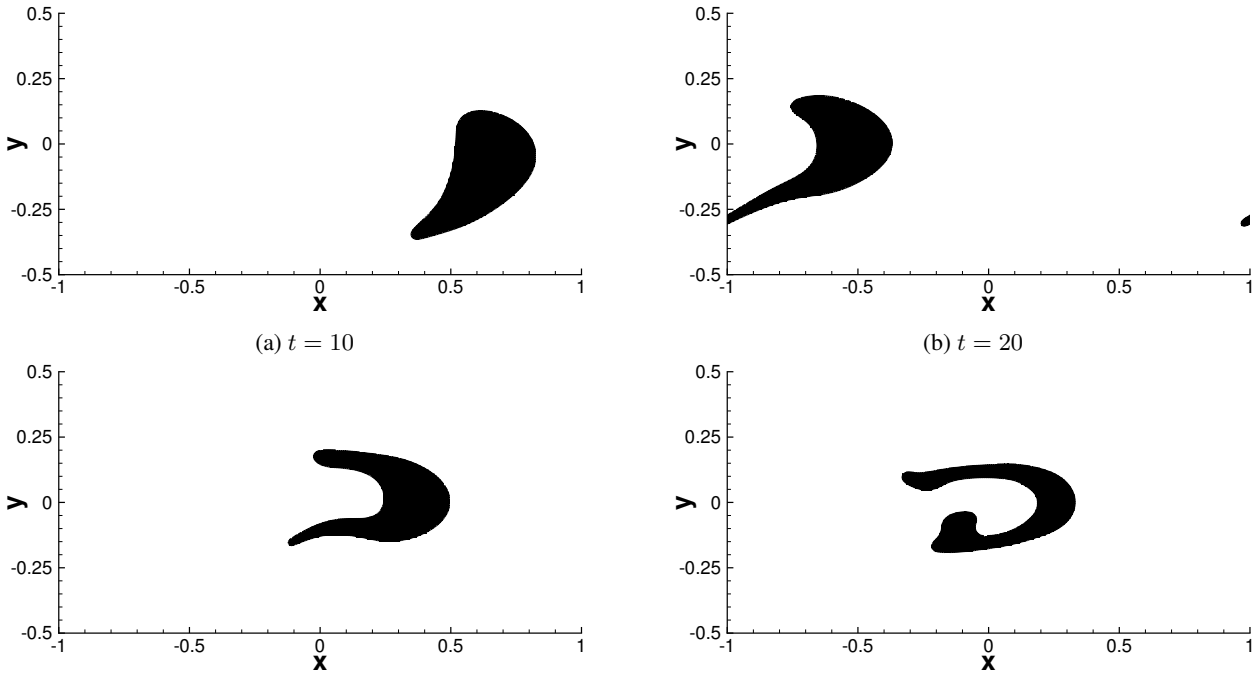

(a) $t = 10$ (b) $t = 20$

(c) $t = 30$ (d) $t = 50$

Figure 7: Droplet deformation on various timesteps for $Ca_{mag} = 1$

where $\mathbf{x}_{cg} = (x_{cg}, y_{cg})$. The denominator of Eq. (26) is the area of the droplet. This allows us to analyze de motion of one single point, however this method does not account for the deformation of the droplet.

Figure 8 shows the vertical position of the droplet's center of mass with respect to time for various Ca_{mag}. For $Ca_{mag} = 0$ (no magnetic field) the droplet migrates towards the centerline as expected. It overshoots the center and gently oscillates until it reaches a steady state. As the magnetic Capillary number increases, the center of gravity moves faster towards the center, however the overshooting decreases. Two factor can explain this phenomena, first we can assume that the deformation caused by the magnetic field puts some of the droplet in regions of higher velocity gradients, which is responsible for the migration. The second factor is that the deformation from the magnetic field itself is responsible for moving the center of gravity.

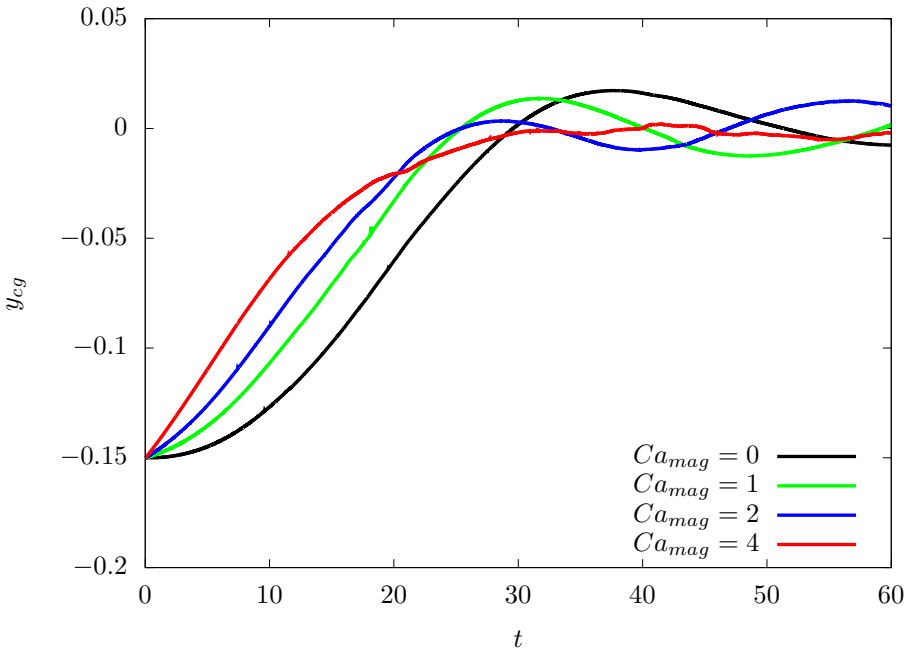

Figure 8: Vertical motion of droplet's center of mass in time with various Ca_{mag}.

The magnetic capillary number also influences the damping of the oscillation. Higher Ca_{mag} creates smaller oscillation in the centerline. For $Ca_{mag} = 4$ the oscillation is minimum, however there are some fluctuations probably created by the magnetic field influence.

5. CONCLUSIONS

In this work, we presented a computational analysis of the motion of a ferrofluid emulsion, consisting of a ferrofluid droplet immersed in a nonmagnetizable fluid under pressure drive flow, with external, an uniform magnetic field applied in the vertical direction. We solve the incompressible Navier-Stokes equations with finite differences discretization and Crank-Nicholson method for temporal evolution. The interface is tracked using the level set method.

It is observed that the droplet migrates towards the centerline of the channel even without the presence of magnetic field. This is due to the effect that the droplet tends to migrate to regions where the velocity gradient is the local minimum. As the magnetic capillary increases, the droplet migrates faster, with less overshooting and oscillations. This can be explained by two factor, the first is that the deformation caused by the magnetic field puts some of the droplet in regions of higher velocity gradient and the second is that the deformation itself is responsible for moving the center of gravity. We must keep in mind that the motion of the center of gravity does not provides means to analyze the deformation.

The future work of our research will be to investigate the influence of the starting point of the droplet, and vary the Capillary and Reynolds numbers. Also changing the external magnetic field direction.

6. ACKNOWLEDGEMENTS

The authors would like to thank Rodrigo Figueiredo Abdo for his valuable insights in this work.

7. REFERENCES

Ahn, K., Kerbage, C., Hunt, T.P., Westervelt, R., Link, D.R. and Weitz, D.A., 2006. "Dielectrophoretic manipulation of drops for high-speed microfluidic sorting devices". *Applied Physics Letters*, Vol. 88, No. 2, p. 024104.

Brown, D.L., Cortez, R. and Minion, M.L., 2001. "Accurate projection methods for the incompressible navier–stokes equations". *Journal of computational physics*, Vol. 168, No. 2, pp. 464–499.

Cox, R. and Brenner, H., 1968. "The lateral migration of solid particles in poiseuille flow—i theory". *Chemical Engineering Science*, Vol. 23, No. 2, pp. 147–173.

Cox, R. and Hsu, S., 1977. "The lateral migration of solid particles in a laminar flow near a plane". *International Journal of Multiphase Flow*, Vol. 3, No. 3, pp. 201–222.

Cunha, F. and Sobral, Y., 2004. "Characterization of the physical parameters in a process of magnetic separation and pressure-driven flow of a magnetic fluid". *Physica A: Statistical Mechanics and its Applications*, Vol. 343, pp. 36–64.

Das, S., Mandal, S. and Chakraborty, S., 2018. "Effect of transverse temperature gradient on the migration of a deformable droplet in a poiseuille flow". *Journal of Fluid Mechanics*, Vol. 850, pp. 1142–1171.

Hazra, S., Malik, L., Mitra, S. and Sen, A., 2022. "Interaction between droplets and co-flow interface in a microchannel: Droplet migration and interfacial deformation". *Physical Review Fluids*, Vol. 7, No. 5, p. 054201.

Hood, K., Lee, S. and Roper, M., 2013. "Inertial migration of a rigid sphere in three-dimensional poiseuille flow". *arXiv preprint arXiv:1312.4653*.

Kaoui, B., Ristow, G., Cantat, I., Misbah, C. and Zimmermann, W., 2008. "Lateral migration of a two-dimensional vesicle in unbounded poiseuille flow". *Physical Review E*, Vol. 77, No. 2, p. 021903.

Kim, J. and Moin, P., 1985. "Application of a fractional-step method to incompressible navier-stokes equations". *Journal of computational physics*, Vol. 59, No. 2, pp. 308–323.

Liu, H., Valocchi, A.J., Zhang, Y. and Kang, Q., 2013. "Phase-field-based lattice boltzmann finite-difference model for simulating thermocapillary flows". *Physical Review E*, Vol. 87, No. 1, p. 013010.

Liu, H., Zhang, Y. and Valocchi, A.J., 2012. "Modeling and simulation of thermocapillary flows using lattice boltzmann method". *Journal of Computational Physics*, Vol. 231, No. 12, pp. 4433–4453.

Mandal, S., Bandopadhyay, A. and Chakraborty, S., 2016. "Dielectrophoresis of a surfactant-laden viscous drop". *Physics of Fluids*, Vol. 28, No. 6, p. 062006.

Mortazavi, S. and Tryggvason, G., 2000. "A numerical study of the motion of drops in poiseuille flow. part 1. lateral migration of one drop". *Journal of Fluid Mechanics*, Vol. 411, pp. 325–350.

Olbricht, W., 1996. "Pore-scale prototypes of multiphase flow in porous media". *Annual review of fluid mechanics*, Vol. 28, No. 1, pp. 187–213.

Seemann, R., Brinkmann, M., Pfohl, T. and Herminghaus, S., 2011. "Droplet based microfluidics". *Reports on progress in physics*, Vol. 75, No. 1, p. 016601.

Skalak, R., Ozkaya, N. and Skalak, T.C., 1989. "Biofluid mechanics". *Annual review of fluid mechanics*, Vol. 21, No. 1, pp. 167–200.

Sussman, M. and Fatemi, E., 1999. "An efficient, interface-preserving level set redistancing algorithm and its application to interfacial incompressible fluid flow". *SIAM Journal on scientific computing*, Vol. 20, No. 4, pp. 1165–1191.

Sussman, M., Fatemi, E., Smereka, P. and Osher, S., 1998. "An improved level set method for incompressible two-phase flows". *Computers & Fluids*, Vol. 27, No. 5-6, pp. 663–680.

Torres-Díaz, I. and Rinaldi, C., 2014. "Recent progress in ferrofluids research: novel applications of magnetically controllable and tunable fluids". *Soft matter*, Vol. 10, No. 43, pp. 8584–8602.

Young, N., Goldstein, J. and Block, M.J., 1959. "The motion of bubbles in a vertical temperature gradient". *Journal of Fluid Mechanics*, Vol. 6, No. 3, pp. 350–356.

8. RESPONSIBILITY NOTICE

The authors are solely responsible for the printed material included in this paper.